BEST: International Journal of Management, Information Technology and Engineering (BEST: IJMITE)
ISSN(Print):2348-0513; ISSN(Online): 2454-471X;
Vol. 3, Issue 9, Sep 2015, 37-52

INTERPRETATION OF $^{16}O(D, \alpha)^{14}N$-REACTION'S MECHANISM AT E_D = 1.876 - 40 MEV

S. E. ABDEL-KARIEM[1] & M. H. KHALIL[2]

Department of Physics, Faculty of Science, Ain-Shams University, Abbassia, Cairo, Egypt

ABSTRACT

The experimental differential cross-sections data for the lower four ^{14}N-states, measured at different twenty deuteron's incident energies ranged from 1.876 to 40 MeV, are used to interpret the mechanism of the $^{16}O(d, \alpha)$-reaction. The zero-range Distorted Wave Born Approximation (DWBA)-Theory with the help of the Cohen-Kurath's spectroscopic factor amplitudes for two-nucleon transfer are used to analyze the experimental data. The experimental angular distributions for the lower two ^{14}N-states G. S. (1^+; 0) and 3.948 MeV (1^+; 0), at lower incident energies (E_d from 1.876 to 18.1 MeV), are incident energy dependent. While those for the four ^{14}N-states G. S. (1^+; 0); 3.948 (1^+; 0); 7.029 (2^+; 0) and 11.05 MeV (3^+; 0), at higher incident energies $E_d \geq 18.8$ MeV, are incident energy independent and they show satisfactory fits with the corresponding theoretical predictions for both the two methods of analysis. On other hand, the experimental forward integrated cross-sections [σ_{exp} (0°-90°)], for the same lower four ^{14}N-states at E_d = 40 MeV, show excellent fits with the bare Cohen-Kurath's SU(3) spectroscopic factors (S) and also with the corresponding theoretical forward integrated cross-sections [$\sigma_{DW\text{-}4}$ (0°-90°) for both semi-microscopic and microscopic]. These satisfactory fits serve as tests for the accuracy of the target and final-nucleus wave functions used in the calculation of spectroscopic-factors. In addition, the experimental forward integrated cross-sections for the lower three ^{14}N-states G. S.; 3.948 and 7.029 MeV, decreases exponentially with increased incident energy and provide good fits with the corresponding theoretical forward integrated cross-section curves. Such fits support the fact that the reaction mechanism, at the higher incident energies ($E_d \geq 18.8$ MeV), is primarily direct. The Cohen-Kurath's theoretical excitation-energies for the lower four ^{14}N-states G. S.; 3.948; 7.029 and 11.05 MeV, can predict and are in excellent agreement with the corresponding experimental values. The accurate prediction for the lower ^{14}N-states is a success of the Cohen-Kurath's wave functions to describe the 1p-shell nuclei and for their model of calculation.

KEYWORDS: Spectroscopic-Factor Amplitudes, Transferred Pair Nucleons,Semi-Microscopic and Microscopi DWBA-Theoretical Analysis

INTRODUCTION

The two-particles transfer nuclear reactions on the 1p- shell nuclei[1-3], using the zero-range Distorted Wave Born Approximation (DWBA)-Theory[4] with two different methods of calculation (semi-microscopic and microscopic), with the help of the Cohen-Kurath's spectroscopic-factor amplitudes (Sp. Fa.) for two particles transfer on the 1p-shell-nuclei[5] were done. Both of the DWBA-theory and the Cohen-Kurath's spectroscopic-factors were used successfully in the theoretical analysis of experimental data and in the interpretation of the mechanism of picked-up reactions such as (d, α)[1,2] and (p, ^{3}He)[3] on 1p-shell nuclei and their inverse reactions. In the semi-microscopic method of calculation, the transferred deuteron is considered as a cluster without internal structure, picked-up from the 1p-shell with orbital angular momentum

quantum number equals 0 or 2 and has spin S = 1. While in the microscopic method, the transferred deuteron considered to transfer as two separated nucleons, each one of them has its private set of quantum numbers.

Previously, in our studies of nuclear reactions, which ended with an alpha-particle as ejectile such as (d, α)[1-3] and (p, α)[6-12], the reaction-mechanism begins to change from the compound nucleus mechanism to the direct one at "definite (critical) incident energy". The value of critical incident energy for a certain reaction is depend on the reaction type and target-structure. The critical energy for a certain reaction, is that corresponds to the formation of the compound nucleus with excitation energy greater than the threshold separation energy of the ejected α-particle from it by ~ 20 MeV[1,2,6-8,11,12].

The ^{16}O(d, α)^{14}N-reaction at some lower incident energies in the range E_d = 1.876 ~ 13.935 MeV were studied[13] .The same reaction were studied[14] at E_d = 15 MeV and at different eleven incident energies ranged from 14.7 to 19.6 MeV[15-17].

Pehl et al.[18] has studied the same reaction at E_d = 24MeV[18] and 40 MeV[19,20].

The aim of this article is to study the mechanism of the ^{16}O(d, α)-reaction at different twenty incident energies ranged from 1.876 to 40 MeV. We used three methods for the nuclear- reaction mechanism interpretation. The first method is fitting the experimental angular-distribution forms for each rest-nucleus state with the corresponding DWBA-theoretical predictions at different incident energies. The second method is comparing the experimental forward integrated cross-sections [σ_{exp} (0°-90°)] with the three values, (2I+1); the theoretical forward integrated cross-sections [σ_{DW4} (0°-90°) for the two methods of calculation]; and with the bare spectroscopic factor S. The third method is by studying the incident energy dependence for both of angular-distribution forms and experimental forward integrated cross-sections for each state at different incident energies associated to each state.

THE THEORETICAL ANALYSIS FORMULA

The Optical Model Parameters

Our analysis for the ^{16}O(d, α)^{14}N-reaction is performed by using the DWBA-theory's (DWUCK-IV)-program[4]. The optical potential parameters used for the incident, outgoing channel and those for the bound-state obtained from literatures. The total potential including all parameters for a certain channel has the form:

$$U = V_c(r_c) - V_o\, f(x_o) + \left(\frac{\hbar}{m_\pi c}\right)^2 \cdot V_{LS}\ (L\cdot\sigma)\cdot\frac{1}{r}\cdot\frac{d}{dr} f(x_{LS}) - i\left[W_v \cdot f(x_v) - 4W_D \frac{d}{dx_D} f(x_D)\right] \qquad (1)$$

where, V_c (r_c) is the Coulomb potential, V_o is the depth of the volume term and V_{LS} is that of the spin-orbit term for the real part of the potential. W_v refer to the depth of the volume term and W_D denote the depth of the surface term for the imaginary part of the potential. f (x_i) stands for the radial function of a Woods-Saxon potential, which is given by:

$$f(x_i) = (1 - e^{x_i})^{-1} \qquad (2)$$

with $x_i = (r - r_i A^{1/3})/a_i$, where r_i, a_i and A are the radius parameter, the diffuseness parameter and the atomic mass number respectively. f (x_i) is a function used to calculate the radial parts for the different potential terms.

The optical parameters used for both of the incident channel (^{16}O+d) and bound state (^{14}N+d), are those obtained by Cooper et al.[20] and Satchler[21] respectively. Cooper et al. have measured the angular distributions for deuteron-^{16}O

elastic scattering at energies of 25.4, 36.0 and 63.2 MeV and their potential is found to be consistent with other data taken in the energy range from 25 to 82 MeV**.** The parameters for the out-going channel (α-particles on ^{14}N) are investigated by Gaillard et al.[22] from the analysis of the elastic scattering of α-particles with incident energy 56 MeV on ^{12}C. By using both of the SUCH-[23] and GOMFIL-program[24], we have modified, the radius and diffuseness parameters for all terms in the three channels. The original and modified parameter-sets for the three channels found in Table 1.

Table 1: The Parameters of Optical Potential Used in $^{16}O(D, \alpha)^{14}N$ Reaction. The Potential Depths Given in (Mev) and the Radii and Diffuseness are in (Fm)

Channel	$^{16}O + d$ [20]		$^{14}N + d$ [21]		$^{14}N + \alpha$ [22]	
	Original	**Modified**	**Original**	**Modified**	**Original**	**Modified**
V_o **	94.79	94.79	87.8	87.8	216.8	216.8
r_o	1.05	1.28889	1.051	1.2094	1.3	1.66153
a_o	0.843	0.702967	0.635	0.38026	0.58	0.276925
W_v	----------	----------	----------	----------	28.05	28.05
r_v	----------	----------	----------	----------	1.5	0.84956
a_v	----------	----------	----------	----------	0.32	0.831596
W_D	8.58	8.58	6.1	----------	----------	----------
r_D	1.573	0.811121	0.935	----------	----------	----------
a_D	0.573	0.769553	1.005	----------	----------	----------
V_{LS}	6.98	6.98	----------	----------	----------	----------
r_{LS}	1.05	1.47753	----------	----------	----------	----------
a_{LS}	0.843	0.836349	----------	----------	----------	----------
r_c	1.3	1.3	1.3	1.3	1.4	1.4

(**) The abbreviations used in the first column have the following descriptions: V_o and V_{LS} are the depths of the volume and spin-orbit terms of the real part of the potential, respectively. W_v and W_D are the depths of the volume and surface terms of the imaginary part of the potential, respectively. The r_i and a_i are the radius and the diffuseness parameters for the (i)-term of potential and r_c is the radius of the Coulomb potential.

Theoretical Analysis

To analyze the experimental data for $^{16}O(d, \alpha)^{14}N$-reaction, we have used two different methods. Firstly, the cluster method, where the cluster transfer form factors were calculated assuming the deuteron to be bound to the residual nucleus in a real Woods-Saxon potential having a radius of 1.2094 fm, diffuse-ness of 0.38026 fm and a depth constrained to fit the binding energy and a Coulomb radius parameter of 1.3 fm were used in all cases. Secondly, the two-particle method, where the form factor calculations were performed using the Bayman and Kallio method[25] using the two-particle coefficients of fractional paren-tage calculated by Cohen and Kurath[5]. In the last method of calculation, each transferred nucleon, assumed bound in Woods-Saxon well with half the binding energy of the transferred deuteron. The optical parameters for both the incident and out-going channels are the same as in the cluster case, while for the bound state, we use the one-particle optical parameters given by Bear and Hodgson; Hodgson[26] (Table 2).

Table 2: Parameters for the One-Particle Optical Potential[26]

$V_\circ$ (MeV)	$r_\circ$ (fm)	$a_\circ$ (fm)	V_{LS} (MeV)	r_{LS} (fm)	a_{LS} (fm)	r_c (fm)
55.7	**1.236**	**0.62**	**7.0**	**1.236**	**0.65**	**1.236**

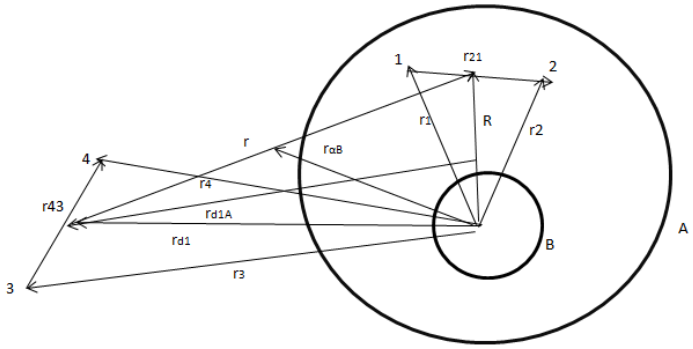

Figure 1: The Coordinates For The Reaction A(d, α)B

THE SEMI-MICROSCOPIC THEORETICAL FORMULA

The Differential Cross Section Formula

The DWBA-theoretical formula for the differential cross section for the pick-up reaction A(d, α)B, by using non polarized projectile and target, is given as[27]:

$$\frac{d\sigma}{d\Omega}(d,\alpha) = \frac{\mu_{d_1 A}\mu_{\alpha B}}{(2\pi\hbar^2)^2}\left(\frac{k_\alpha}{k_{d_1}}\right)\frac{1}{[(2J_A+1).(2s_{d_1}+1)]}\sum_{M_A M_B M_{d_2}}\left|T^{DWBA}_{(d,\alpha)}\right|^2 \qquad (3)$$

where $\mu_{d_1 A}$ (k_{d_1}) and $\mu_{\alpha B}$ (k_α) are the reduced masses (wave numbers) in the initial and final channels, respectively; s_{d_1} and J_A are the spins of the incident deuteron and target nucleus (A), respectively. M_A, M_B and M_{d2} are the target, rest nucleus and ejected particle magnetic quantum number respectively.

$T^{DWBA}_{(d,\alpha)}$ is the reaction transition amplitude, which has the following form according to the DWBA theory

$$T^{DWBA}_{(d,\alpha)}(A,B) = \iint d\underline{R}\, d\underline{r}\,.\,\chi^{(-)^*}(\underline{k}_\alpha, \underline{r}_{\alpha B}).\left\langle \Psi_\alpha \Psi_B \left| V \right| \Psi_A \Psi_{d_1} \right\rangle^a .\chi^{(+)}(\underline{k}_{d1}, \underline{r}_{d1A}) \qquad (4)$$

Where, $\chi^{(+)}(\underline{k}_{d_1}, \underline{r}_{d_1 A})$ and $\chi^{(-)^*}(\underline{k}_\alpha, \underline{r}_{\alpha B})$ are the distorted waves for the elastic scattering due to optical potentials in the initial- and final channel, respectively. The integration in this formula is performed on the center of mass $\underline{R}$ =1/2 ($\underline{r}_1$ + $\underline{r}_2$) and on the relative coordinate $r = 1/2\,(\underline{r}_1 + \underline{r}_2) - \underline{r}_{d1}$, where $\underline{r}_1$ and $\underline{r}_2$ are the coordinates for both of the two individual transferred particles and $\underline{r}_{d1}$ is that for the incident deuteron (Fig. 1). These three coordinates of the three particles refer to the center of the rest-nucleus in the reaction (B). The quantity found as a bracket $\left\langle \Psi_\alpha \Psi_B \left| V \right| \Psi_A \Psi_{d1} \right\rangle^a$ is the anti symmetric nuclear matrix element and it can write as follows:

$$\left\langle \Psi_\alpha \Psi_B \left| V \right| \Psi_A \Psi_{d1} \right\rangle^a = \binom{4}{2}^{1/2}.\binom{A}{2}^{1/2}.\left\langle \Psi^a_\alpha \Psi^a_B \left| V \right| \Psi^a_A \Psi^a_{d1} \right\rangle \qquad (5)$$

This bracket is dependent on the four wave functions (Ψ^a_{d1}), (Ψ^a_{α}), (Ψ^a_{A}) and (Ψ^a_{B}) for projectile, ejectile, target and rest nucleus, respectively; and the two binomial coefficients $\binom{4}{2}^{1/2}$ and $\binom{A}{2}^{1/2}$ are obtained from the anti symmetry.

In the two previous papers[2], we have derive the microscopic formula for the differential cross-section and in our present paper, we will try to derive the semi-microscopic formula for the differential cross-section. In the semi-microscopic calculation, a cluster form factor used together with the cluster spectroscopic amplitudes, which can obtain with the help of a microscopic method of calculation. In the cluster approxi-mation, both of projectile and transferred deuteron considered as point-particles and they have no internal structure. This leads to a formula for the target wave function has the form:

$$\hat{\Psi}^a_A(\xi_A) = \binom{A}{2}^{-1/2} \sum_{\substack{J J_B \\ T T_B}} \sum_{L S} \hat{S}^{1/2}_{AB}(L S J T) \cdot \left[\Psi^a_B(\xi_B)^{J_B T_B} \times \hat{\Psi}_{d2}(\xi_{d2})^{L S J T} \right]^{J_A T_A}_{M_A N_A} \quad (6)$$

In the case of (d, α)-reactions, the form of the interaction potential V presented in the nuclear matrix element (eq. 5), is that between the incident (d1) and the transferred deuteron (d2) and it can write as follows:

$$\hat{V} = V_{d1\, d2}(\underline{r}) \quad (7)$$

The ejected α-particle wave function has the form:

$$\hat{\Psi}_{\alpha}(\xi_{\alpha}) = \varphi_{\alpha}(\underline{r})^{L_{\alpha}=0}_{M_{L_{\alpha}}=0} \cdot \chi^a_{\alpha}(\sigma_{\alpha}, \tau_{\alpha})^{S_{\alpha}=T_{\alpha}=0}_{M_{S_{\alpha}}=N_{\alpha}=0} \quad (8)$$

The wave function for the transferred deuteron-cluster given by:

$$\hat{\Psi}_{d2}(\xi_{d2}) = \sum_{M_{L_{d2}} M_{S_{d2}}} (L_{d2}\, M_{L_{d2}}\, S_{d2}\, M_{S_{d2}} | J M)\, \varphi_{d2}(\underline{R})^{L_{d2}\, J_{d2}}_{M_{L_{d2}}} \cdot \chi(\sigma_{d2}, \tau_{d2})^{S_{d2}=1\, T_{d2}=0}_{M_{S_{d2}}\, N_{d2}=0} \quad (9)$$

The summation over $M_{L_{d2}}$ and $M_{S_{d2}}$ for the transferred deuteron vanished in the case of the transition amplitude, because $M_{S_{d2}} = -M_{d2}$ and $M_{L_{d2}} = M + M_{d2}$.

Inserting the formula for the equations (6) to (9) in equation (5) and by substituting in eq. (4), then the final formula for the semi-microscopic transition amplitude has the form:

$$T^{DWBA}_{(d,\alpha)}(A, B) = \sum_{J M} (J_B\, M_B\, J M | J_A\, M_A)(T_B\, N_B\, T N | T_A\, N_A) \cdot \sum_{L_{d2}} (L_{d2}\, (M + M_{d2})\, 1\, (-M_{d2}) | J M) \cdot D(S, T)$$
$$\cdot (1\, M_{d1}\, (-M_{d2}) | 0\, 0) \cdot b_{S T} \cdot \hat{S}^{1/2}_{AB}(L S J T) \cdot \iint d\underline{R}\, d\underline{r} \cdot \chi^{(-)*}(\underline{k}_{\alpha}, \underline{r}_{\alpha B}) \cdot \hat{F}^{L_{d2}\, J}_{M_{L_{d2}}}(\underline{R}, \underline{r}) \cdot \chi^{(+)}(\underline{k}_{d1}, \underline{r}_{d1 A})$$
$$\cdot \quad \text{..... .... (10)}$$

where, T_A, T_B and N_A, N_B are the isospin quantum numbers and their z-components for the target and rest nucleus respectively. The two brackets $(J_B\, M_B\, J M | J_A\, M_A)$ and $(T_B\, N_B\, T N | T_A\, N_A)$ represent the Clebsch-Gordon

coefficients and the quantity $\hat{S}_{AB}^{1/2}(L\,S\,J\,T)$ is the semi-microscopic spectroscopic factor amplitude. The Clebsch-Gordon coefficient $\left(1\,M_{d1}\,1\left(-M_{d2}\right)\,|\,0\,0\right)$ couples the spin for projectile with that of the transferred deuteron to give the spin of ejected α-particle. The quantity $b_{S\,T}$ is the spectroscopic amplitude for the light particle, and it can calculate as follows:

$$b_{S\,T} = (-1)^{m\alpha+1}\begin{pmatrix}4\\2\end{pmatrix}^{1/2}\cdot\frac{1}{\sqrt{2}}.\delta_{S+T,1}.\left(T_d\ N_d\ T\ N\,|T_\alpha\ N_\alpha\right) = -\frac{\sqrt{6}}{\sqrt{2}}\left(0\,0\,0\,0|0\,0\right) = -\sqrt{3} \qquad (11)$$

D (S, T) found in eq. (10) is a quantity, which distinguishes the different strengths of the interaction potential for $\hat{F}_{M_{L_{d2}}}^{L_{d2}\,J}(\underline{R},\underline{r})$ the singlet and triplet states and L_{d2} is the form factor for the semi-microscopic case, which given by formula:

$$\hat{F}_{M_{L_{d2}}}^{L_{d2}\,J}(\underline{R},\underline{r}) = \left\langle \varphi_\alpha(\underline{r})_0^0 \left| V_{d1d2}(\underline{r}) \right| \varphi_{d2}(\underline{R})_{M_{L_{d2}}}^{L_{d2}\,J} \right\rangle = D^{(d,\alpha)}(\underline{r})\ .\ \varphi_{d2}(\underline{R})_{M_{L_{d2}}}^{L_{d2}\,J} \qquad (12)$$

where $\varphi_{d2}(\underline{R})_{M_{L_{d2}}}^{L_{d2}\,J}$ is the radial wave function for the transferred deuteron-cluster, which is calculated in a Woods-Saxon potential. In the zero-range approximation, we replace $D^{(d,\alpha)}(\underline{r})\ by\ D_\circ^{(d,\alpha)}\,.\,\delta(\underline{r})$, and then the form factor has the form

$$\hat{F}_{M_{L_{d2}}}^{L_{d2}\,J}(\underline{R}) \approx D_\circ^{(d,\alpha)}(\underline{r})\,.\,\varphi_{d2}(\underline{R})_{M_{L_{d2}}}^{L_{d2}\,J} \qquad (13)$$

By comparing the two formula for microscopic[1,2)] and cluster form factors together, one can see, which approximation in the microscopic model leads quickly to the cluster form and finally this leads to get the conservation of the Oscillator-quantum numbers as follows:

$$2n_1 + \ell_1 + 2n_2 + \ell_2 = 2N + L = Q \qquad (14)$$

In the microscopic case, the wave functions for the transferred pair of nucleons can transfer in the relative and center of mass coordinates and $(n_1,\ell_1)\ and\ (n_2,\ell_2)$, are the special quantum numbers and orbital angular momentum for each one of the two transferred particles (1 and 2), (N, L) are those for the center of mass motion for the two transferred nucleons, respectively. Q is the total oscillator quantum numbers.

According eq. (12), the microscopic form factor transformed to the cluster form factor, by replacing the Harmonic Oscillator wave function $\Phi(\underline{R})_{M_L}^{N'L}$ by the Woods-Saxon wave function $\varphi_{d2}(\underline{R})_{M_{L_{d2}}}^{L_{d2}\,J}$ [1,2)]. By using this approximation, the final formula for the differential cross-sections factorized into two separated factors, a structure one $\hat{S}_{AB}^{1/2}(L\,S\,J\,T)$, which measured the strength of the transition under consideration, and a kinematical one

$$\left(\int \chi^{(-)^*} (\underline{k}_\alpha , \underline{r}_{\alpha B}) \cdot \varphi_{d2} (\underline{R})^{L_{d2}}_{M} d\underline{R} \right)^{L \; J}$$

,

which describes the form of angular distribution.

The zero-range DWBA-semi-microscopic differential cross-section for a (d, α)-reaction can calculate by the DWUCK-IV program and in this case, there is a relation between experimental and theoretical cross-section as follows

$$\left(\frac{d\sigma}{d\Omega}\right)_{exp} \frac{\varepsilon^{(d,\alpha)}_{cluster}}{(2S_d+1)} \cdot C^2 \cdot \left[\frac{\left(T_B N_B \, T N \middle| T_A \, N_A\right) \cdot D_o^{(d,\alpha)} \cdot b_{ST}^{(d,\alpha)} \cdot D^{(d,\alpha)}(S,T)}{10^2}\right]^2 \cdot \sum_J \frac{1}{(2J+1)} \left(\frac{d\sigma}{d\Omega}\right)^J_{DWUCK-IV} \quad \text{.....(15)}$$

where, $D_o^{(d,\alpha)} = 715\,MeV \cdot fm^{3/2}$; $b_{ST}^{(d,\alpha)} = -\sqrt{3}$; $D\,(S=1, T=0)^{(d,\alpha)} = 0.5$; $\varepsilon^{(d,\alpha)}_{cluster}$ is the factor describe the deviation between experiment and theory ; the isospin Clebsch-Gordon Coefficient for $^{16}O(d,\alpha)^{14}N$-reaction $\left(T_B N_B \, T N \middle| T_A \, N_A\right) = 1.0$ and $C = g(\rho) \cdot \Omega_d \cdot \left\langle n_1 \ell_1 n_2 \ell_2 : L \middle| N' \, L \, 0 \, 0 : L \right\rangle \approx 1.0$.

Transfer of Microscopic Spectroscopic Factor Amplitudes to Semi-Microscopic

According to the microscopic method of calculation[1,2], the target wave function (Ψ^a_A) can be write as an expansion of the wave functions for the rest nucleus $\left[\Psi^a_B(\xi_B)\right]$ and the transferred pair of nucleons $\left[\Psi^a_x(\xi_1 \xi_2)\right]$ as follows:

$$\Psi^a_A(\xi_A)^{J_A T_A}_{M_A N_A} = \binom{A}{2}^{-1/2} \cdot \sum_{J J_B J_1 J_2} \sum_{T T_B} S^{1/2}_{AB}(\rho JT) \sum_{M M_B N N_B} \left(J_B M_B J M \middle| J_A M_A\right) \left(T_B N_B \, T N \middle| T_A N_A\right) \cdot \Psi^a_B(\xi_B)^{J_B T_B}_{M_B N_B} \cdot \Psi^a_x(\xi_1 \xi_2)^{\rho JT}_{MN} \quad (16)$$

Using this formula, we can obtain a formula for the microscopic spectroscopic amplitude by inversing this equation, as follows:

$$S^{1/2}_{AB}(\rho JT) = \binom{A}{2}^{1/2} \cdot \left\langle \left[\Psi^a_B(\xi_B)^{J_B T_B}_{M_B N_B} \cdot x \Psi^a_x(\xi_1 \xi_2)^{\rho JT}_{MN} \right]^{J_A T_A}_{M_A N_A} \middle| \Psi^a_A(\xi_A)^{J_A T_A}_{M_A N_A} \right\rangle \quad (17)$$

To transfer the microscopic spectroscopic amplitudes to semi-microscopic (shell-model), we use the Moshinsky-transformation[28], in which the coordinates (ξ), which refer to the center of the rest-nucleus (B), changed to another one (ζ), which refer to the center of the shell-model potential. This can simply performed by using a simple approximation, where the deuteron cluster replaces the transferred nucleon-pair wave function and the final form obtained for the semi-microscopic spectroscopic amplitude[29] is:

$$S_{AB}^{1/2}(\rho J T) = \binom{A}{2}^{1/2} \cdot \left(\frac{A}{A-2}\right)^{Q/2} \cdot < \left[\Psi_B^a(\zeta_B)^{J_B T_B}_{M_B N_B} .x\, \Psi_x^a(\zeta_1 \zeta_2)^{\rho J T}_{M N} \right]^{J_A T_A}_{M_A N_A} | \Psi_A^a(\zeta_A)^{J_A T_A}_{M_A N_A} >$$

$$\equiv \binom{A}{2}^{1/2} \cdot \left(\frac{A}{A-2}\right)^{Q/2} \cdot \left\langle \Psi_B^{J_B T_B} \cdot \Psi_x^{\rho J T} \right| \} \left| \Psi_A^{J_A T_A} \right\rangle \qquad (18)$$

Where, $\left(\frac{A}{A-2}\right)^{Q/2}$ is the center of mass correction-factor and Q is the total oscillator quantum number (eq. 14) and the integral $\left\langle \Psi_B^{J_B T_B} \cdot \Psi_x^{\rho J T} \right| \} \left| \Psi_A^{J_A T_A} \right\rangle$ is known as the two-nucleons coefficient of fractional parentage (c. f. p.).

DISCUSSIONS

As we mentioned previously, the mechanism for a certain nuclear reaction, which ended with an alpha particle as ejectile, begins to change from the compound nucleus mechanism to the direct one at definite (critical) incident energy. This incident energy is dependent on both of reaction type and target structure. In addition, the characteristics of the experimental data obtained in a certain nuclear reaction are dependent on its mechanism or on incident energy at which the experimental data are measured. This means that, by studying the characteristics of the experimental data obtained in a certain nuclear reaction at certain incident energy, we can interpret exactly its mechanism. The experimental data found in literatures for the ^{16}O(d, α)^{14}N-reaction, were performed at twenty different incident energies ranged from 1.876 to 40 MeV[13-19]. To interpret the mechanism of this reaction, in this range of incident energy, we use the predictions of zero-range DWBA-theory's program[4] and the Cohen-Kurath's spectroscopic factors[5].

Angular-Distribution Forms in ^{16}O(d, α)^{14}N-Reaction

It is known that, at very low incident energies, the angular-distribution forms are energy dependent. When the incident energy increases until it reached the critical value for a state in a reaction, then begins the stability of its angular distribution and with increasing the incident energy more and more the stability increases until it reached its maximum at certain value for incident energy. This means that, the form of angular-distribution for a transition in a certain reaction is mainly dependent on the dominant mechanism in this reaction and with increasing the ratio of direct mechanism; this increases the stability of its form. The maximum stability of the angular-distribution form reached at certain incident energy, which is dependent on both reaction type and target-structure and its value probably change from a state to another one.

As shown in Fig. (2 A), the forms of ^{14}N-state G. S. (1^+; 0) angular distributions, obtained in the reaction ^{16}O(d, α)^{14}N at low incident energies (E_d = 1.876 ~ 18.1 MeV), are energy dependent. Starting from the next incident energy E_d ~ 18.8 MeV, begins the stability of G. S.-forms and appears a new minimum at the angle $\theta_{C.M.} \sim 30^\circ$. The stability for ^{14}N-state G. S. angular-distributions increases with increasing incident energy in the range E_d = 18.8 – 40 MeV and there are similarity between their forms. Similarly, the angular-distribution forms for the ^{14}N-state 3.948 (1^+; 0) MeV (Fig. 2 B. a and b), obtained at lower incident energies E_d = 14.9 to 18.1 MeV, are energy dependent, while at higher incident energies ranged from E_d = 18.8 to 40 MeV, they have similar forward diffraction forms.

The two angular distributions for the ^{14}N-state 7.029 (2^+; 0) MeV (Fig. 2 B. c), measured at E_d = 24 and 40 MeV, have similar forward diffraction forms. That for the ^{14}N-state 11.05 (3^+; 0) MeV (Fig. 2 B. c), measured at the incident energy E_d = 40 MeV, has a form, which probably due to the dominant of direct mechanism.

Table 3: The Experimental[30] and Calculated Excitation Energies[5] for the First Four ^{14}N- States Obtained in the Reaction $^{16}O(D, A)^{14}N$ Together with the Total Angular Momentum, Isospin, The SU(3) Spectroscopic Factors Amplitudes and total Spectroscopic Factors for the Cluster Case

E_x (MeV)[30]	E_{cal}(MeV)[5]	J^π[30]	Isospin[30]	Spectroscopic Factor Amplitude *[5]				Total Sp. Fa. (S)
				$^3D_3$	$^3D_2$	$^3D_1$	$^3S_1$	
G. S.	0.0	1^+	0	----------	----------	1.64434	- 0.1281	2.72026
3.948	3.62	1^+	0	----------	----------	0.28604	1.63571	2.75737
7.029	6.99	2^+	0	----------	2.236548	----------	----------	5.00215
11.05	10.14	3^+	0	2.646	----------	----------	----------	7.00131

*) The spectroscopic factors amplitudes are normalized to the transferred angular momentum (j) and final isospin.

REACTION-MECHANISM INTERPRETATION

Fits of Angular-Distributions with Theoretical Predictions

Considering the transferred two-nucleons, in the $^{16}O(d, \alpha)^{14}N$-reaction at higher incident energies, are picked-up from the 1p-shell through a direct mechanism. Then, the two different methods of zero-range DWBA-theory[4] (semi-microscopic and microscopic) can be used to calculate the corresponding differen-tial cross-sections for the four lower ^{14}N-states by using both of the modified set of the optical-model parameters [Tables (1) and (2)] and the Cohen-Kurath's spectroscopic factor amplitudes[5] [Table (3)]. Then, the fit of experimental angular distributions with the theoretical predictions used as a method for the reaction-mechanism interpretation as follows:

As shown in Figure (2 A), the ^{14}N-state G. S. (1^+; 0)-angular-distribution forms, obtained at lower incident energies E_d = 1.876 ~ 18.1 MeV, are energy dependent, this due to the dominant of compound nucleus mechanism. While at higher incident energies $E_d \geq$ 18.8 MeV, begins the stability of G. S.- angular-distribution forms and it increases with increasing incident energy, this due to the dominant of direct mechanism in this range. This leads to obtain excellent fits between the G. S.-experimental forms and the DWBA-theoretical predictions for the two methods of analysis in the incident energy range E_d = 18.8 - 40 MeV.

The angular distributions for the ^{14}N-state 3.948 MeV (1^+; 0) (Fig. 2 B. a and b), measured at the higher incident energies (ranged from E_d = 18.1 to 40 MeV), exhibit too the characteristics of direct mechanism. Where they show excellent fits between experimental forms and theoretical predictions, this may due to the dominant of direct mechanism in this incident-energy range. On other hand, at low incident energies E_d = 14.9 to 17.3 MeV, there is no fits between experimental and theoretical forms, which probably due to the dominant of compound nucleus mechanism in this range of incident energy.

The two angular distributions for the ^{14}N-state 7.029 MeV (2^+; 0) (Fig. 2 B. c), measured at E_d = 24 and 40 MeV, have similar forward diffraction forms and show good fits with the DWBA-theoretical predictions, this probably due to the dominant of direct mechanism. The angular distribution for the ^{14}N-state 11.05 (3^+; 0) MeV (Fig. 2 B. c), obtained at the incident energy E_d = 40 MeV, exhibits too the characteristics of direct mechanism and shows good fit with the corresponding DWBA-theoretical predictions, this probably due to the dominant of direct mechanism.

Total Cross Sections

The experimental forward integrated cross-sections [σ_{exp} (0°-90°)], for the lower ^{14}N-states at the two incident energies 24 and 40 MeV, as shown in Fig. (3), are compared with the corresponding values of the three physical quantities: the theoretical forward integrated cross-sections [σ_{DW4} (0°-90°) for both semi-microscopic and microscopic method of calculation] and the total spectroscopic factor S. In this Figure, the experimental forward integrated cross sections σ_{exp} (0° - 90°) show excellent fits with both the bare Cohen-Kurath's[5] spectroscopic factors for two-nucleons transfer [Table (3)] and theoretical forward integrated cross sections [$\sigma_{DW4\ (Cluster\ and\ Microscopic)}$ (0°-90°)] especially at E_d = 40 MeV. Such fits supports the fact that the reaction mechanism at these two higher incident energies is primarily direct[1-3,6,9]. This can considered as a second method for the reaction-mechanism interpretation. The solid- ; dashed-dotted-; short dashed- and dotted lines, plotted in Fig. (3) for a transition, represent its experimental forward integrated cross section [σ_{exp} (0°-90°)]; semi-microscopic- [$\sigma_{DW4\ (Cluster)}$ (0°-90°)]; microscopic forward integrated cross-section [$\sigma_{DW4\ (Microscopic)}$ (0°-90°)] and spectroscopic factors (S), respectively. The fits between the above given four values for each ^{14}N-state at E_d = 40 MeV as shown in Fig. (3), is very excellent in comparison with that at E_d = 24 MeV. These because at higher incident energy, the reaction mechanism is pure direct, while at lower energy, the ratio of direct mechanism probably is weak.

Incident Energy Dependence for the Forward Total Cross Sections

As a last method for the reaction-mechanism interpretation, we compare the experimental forward integrated cross-sections σ_{exp} (0°-90°), for each one of the three ^{14}N-states G. S. (1^+; 0); 3.948 (1^+; 0) and 7.029 (2^+; 0) MeV, with the corresponding two theoretical values $\sigma_{DW4\ (semi\text{-}microscopic\ and\ microscopic)}$ (0° - 90°) in the incident energy range associated to each state [Fig. 4]. As shown in Figure (4), excellent fits are obtained between the above maintained three values and the three curves for the forward cross-sections for each state decreases exponentially, with increasing incident energy, this is a characteristic for the direct mechanism.

Table 4: The Experimental[30] and Theoretical[5] Energy Levels for the ^{14}N Nucleus in the ^{16}O(d,α)^{14}N Reaction

Level Angular Momentum and Isospin (J^{π} ; T)[30]	Energy Level E_x (MeV)	
	Experimental[30]	Theoretical[5]
1^+; 0	G. S.	0.00
1^+; 0	3.948	3.62
2^+; 0	7.029	6.99
3^+; 0	11.05	10.14

Excitation Energies

The theoretical values of excitation-energies for the lower four ^{14}N-states G. S. (1^+; 0); 3.948 (1^+; 0); 7.029 (2^+; 0) and 11.05 (3^+; 0) MeV, calculated by Cohen and Kurath[5], are in excellent agreement with the corresponding experimental values[30] [both are presented in Table (4) and Fig. (5)]. Cohen-Kurath have used their wave functions[31, 32] in the calculation of the theoretical excitation energies and they could accurately predict the above given lower four ^{14}N-states. This can consider as a success of their wave functions and model of calculation to describe the 1p-shell nuclei.

CONCLUSIONS

The aim of our present study is to interpret the mechanism of the $^{16}O(d, \alpha)^{14}N$-reaction at E_d ranged from 1.876 to 40 MeV. At higher incident energies, we have used both of the semi-microscopic and microscopic zero-range DWBA-theory[4] to calculate the theoretical differential cross sections for the lower four ^{14}N-states G. S. (1^+; 0); 3.948 (1^+; 0); 7.029 (2^+; 0) and 11.05 (3^+; 0) MeV. In our semi-micros-copic analysis, we have used three modified sets of the optical-model parameters for the three channels and the Cohen-Kurath's spectroscopic-factor amplitudes[5]. In the semi-microscopic method, the transferred deuteron is considered as a cluster without internal structure, picked-up from the 1p-shell with orbital angular momentum quantum number equals 0 or 2 and has spin S = 1. While in the microscopic method the transferred deuteron considered to transfer as two separated nucleons, each one of them has its private quantum number set. The results of our analysis for the lower four ^{14}N-states G. S. (1^+; 0); 3.948 (1^+; 0); 7.029 (2^+; 0) and 11.05 (3^+; 0) MeV, can be summarize as follows:

- The experimental angular-distribution forms for the first two ^{14}N-states G. S. (1^+; 0) and 3.948 (1^+; 0) MeV, obtained in the incident energy range E_d = 1.876 to 18.1 MeV, are incident energy dependent. While in the higher incident energy range E_d = 18.8 ~ 40 MeV, their angular distribution forms are stable and show good fits with the corresponding zero-range DWBA theoretical predictions (Fig. 2 A. d and 2 B. b and c).
- The experimental forward integrated cross sections $\sigma_{exp}(0° - 90°)$, obtained at E_d = 40 MeV for the above given lower four ^{14}N-states, show excellent fits with both the bare Cohen-Kurath's SU(3) spectroscopic factors and the theoretical forward integrated cross sections for the two different methods of calculations [$\sigma_{semi\text{-}microscopic}$ (0°-90°) and $\sigma_{microscopic}$ (0°-90°)] (Fig. 3). While at E_d = 24 MeV, the fits between the four physical quantities for the lower three ^{14}N-states is not satisfactory.
- The experimental forward integrated cross-sections, for the lower three ^{14}N-states G. S. (1^+; 0), 3.948 (1^+; 0) and 7.029 (2^+; 0) MeV, decrease exponentially with incident energy, and provide good fits with the corresponding theoretical forward integrated cross-section curves (Fig. 4). Such fits support the fact that the reaction mechanism is primarily direct[1-3]. This process begins for ^{14}N- G. S. (1^+; 0) at E_d ~ 18 MeV and for the other two states begins at E_d ~ 24 MeV.
- Cohen and Kurath have used their wave-functions[31,32] to calculate the theoretical excitation energies for the lower four ^{14}N-states which were in excellent agreement with the corresponding experimental values[30] [see Table (4) and Fig. (5)]. This means that, the accurate prediction for excitation energies of the above given lower four ^{14}N-states is a success of their wave functions to describe the 1p-shell nuclei and too for their model of calculation.

REFERENCES

1. S. E. Abdel-Kariem, Doctor thesis, Tuebingen University, (1984).
2. S. E. Abdel-Kariem and G. Staudt, "**Microscopic and Semi-microscopic Analysis for the $^{12}C(d, \alpha)^{10}B$-Reaction at E_d = 9.2 - 40 MeV**" and S. E. Abdel-Kariem and M. H. Khalil, "**DWBA-Theory for Deuteron Pick-up and Analysis for The $^{14}N(d, \alpha)^{12}C$-Reaction at E_d = 10.5 - 40 MeV"** to be published.
3. V. Rapp, Doctor Thesis, Tuebingen University, (1982).

4. P. D. Kunz, Computer code DWUCK-IV, (Uni. Colorado, Boulder, PC-VERSION ' 12 /Jan /1995').

5. S. Cohen and D. Kurath, Nucl. Phys. A 141, 145 (1970).

6. W. Buck, Doctor thesis, Tuebingen University, 1976 and the references therein;

   A. Staebler, W. Buck, G. Staudt and H. Oeschler, Nucl. Phys. A 275, 269(1977) and

   W. Buck, F. Hoyler, A. Staebler , G. Staudt, H. V. Klapdor and H. Oeschler, Nucl. Phys. A 398, 189 (1983).

7. F. Weng, Doctor thesis, Tuebingen University, 1979;

   F. Weng, M. Moerike, T. Rohwer, G. Staudt and P. Turek, Annual Report 1974, Inst. fuer Kernphysik der KFA-Juelich, 10/ 75 ,P. 40 (1974) and

   F. Weng, T. Rohwer and G. Staudt, Annual Report 1979, Inst. fuer Kernphysik der KFA- Juelich, Jul-Sep. 72,P. 12 (1979).

8. S. E. Abdel-kariem, T. Rohwer, G. Staudt and W. Leitner, Nucl. Phys. A 487, 353 (1988);

   S. E. Abdel-Kariem, Applied Radiation and Isotopes (United Kingdom) 64, 925-933 (2006);

   S. E. Abdel-Kariem, Balkan Physics Letters (Istanbul- Turkey), 14 (1), 12-23 (2006) and

   S. E. Abdel-Kariem, Egyptian Journal of Physics (Cairo University), Vol. 39, No. 1, 25 - 39 (2008).

9. H. -J. Hauser, Diploma thesis, Tuebingen University, 1981;

   H. - J. Hauser, T. Rohwer, F. Hoyler, G. Staudt, S. Abdel-Kariem, P. Grosshoff, H. V. Klapdor, A Korber, W. Leitner, V. Rapp, M. Walz and D. Wienmann, in AIF Conf. (USA); No. 125, 701 (1985) and

   H. - J. Hauser, M. Walz, F. Weng, G. Staudt and P. K. Rath, Nucl. Phys. A 456, 253 (1986).

10. M. Walz, Diploma thesis, Tuebingen University, (1982).

11. F. Hoyler, Doctor thesis, Tuebingen University, (1982).

12. Rohwer, Doctor thesis, Tuebingen University, (1980).

13. P. L. Jolivette, Phys. Rev. C 8, 1230 (1973).

14. F. Pellegrini, Nucl. Phys. 24, 372 (1961).

15. T. Yanabu, Jour. Phys. Soc. Japan 16, 2118 (1961).

16. T. Yanabu, S. Yamashita, T. Nakamura, K. Takamatsu, A. Masaike, S. Kakigi, D. C. Nguyen and K. Takimoto, Jour. Phys. Soc. Japan 18, 747 (1963).

17. G. Freemantle, W. M. Gibson, D. J. Prowse and J. Rotblat, Phys. Rev. 92, 1268 (1953).

18. H. Pehl, J. Cerny, E. Rivet and B. G. Harvey, Phys. Rev. 140, B605 (1965).

19. VAN DER Woude and R. J. DE Meijer, Nucl. Phys. A 258, 199 (1976).

20. D. Cooper, W. P. Hornyak and P. G. Roos, Nucl. Phys. A 218, 249 (1974).

21. G. R. Satchler, Private communication to P. N. Hodgson (1965).

22. P. Gaillard, R. Bouche', L. Feuvrals, M. Gaillard, A. Guichard, M. Gusakow, J. L. Leonhardt and J. R. Pizzi , Nucl. Phys. A 131, 353 (1969).

23. Private communications to nuclear reactions group in Physikalisches Institut, Universitaet Tuebingen, Computer Program SUCH (Unpublished).

24. H. Leeb et al., Universitaet Wien, Computer Program GOMFIL, 2. Version (1980) (Unpublished).

25. F. Bayman and A. Killio, Phys. Rev. 156, 1121 (1967).

26. K. Bear and P. E. Hodgson, J. Phys. G4, L287 (1978) ; P. E. Hodgson, Growth points in nuclear physics, Volume 3, Pergamon Press (1981).

27. N. Austern,"Direct nuclear reaction theories", Wiley, New York, (1970); G. R. Satchler, Nucl. Phys. 55, 1 (1964).

28. I. Talmi, Helv. Phys. Acta 25, 185 (1952);

    M. Moshinsky, Nucl. Phys. 13, 104 (1959);

    YU. F. Smirnov, Nucl. Phys. 27, 177 (1961); 39, 346 (1962) and

    A. De Shalit and I. Talmi, Nucl. Shell theory, P. 238, Academic Press, (1963).

29. M. Ichimura, A. Arima, E. C. Halbert, and T. Terasawa, Nucl. Phys. A204, 225 (1973).

30. D. R. Tilley et al., (F. Ajzenberg-Selove); Nucl. Phys. A 523, 1(1991); TUNL AND FAS Publications, Revised Manuscript of "Energy Levels of Light Nuclei A = 14", Page 27 – 67 (Internet in 19. November 2001).

31. S. Cohen and D. Kurath, Nucl. Phys. 73, 1 (1965).

32. S. Cohen and D. Kurath, Nucl. Phys. A 101, 1 (1967).

APPENDICES

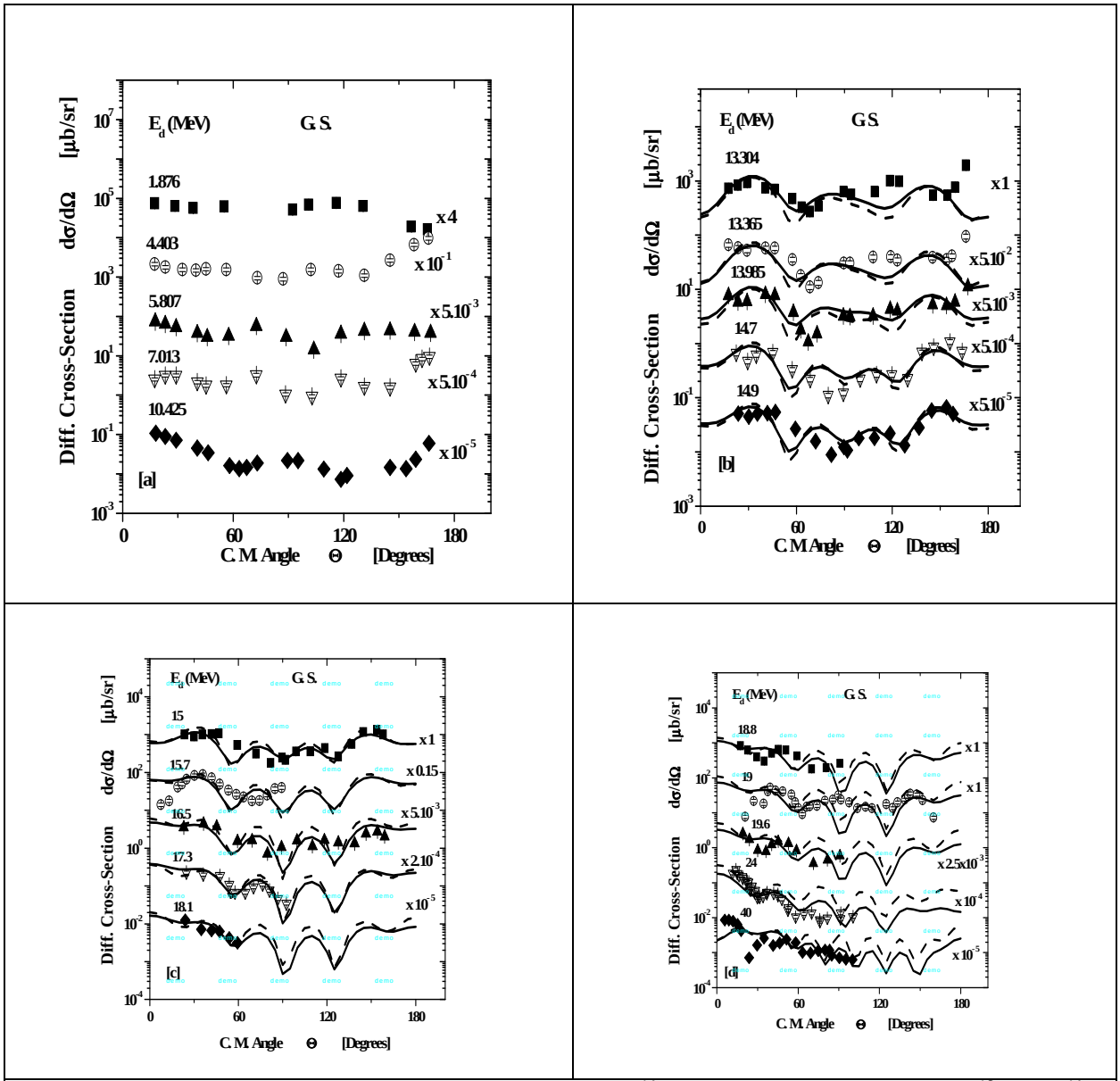

Figure (2 A): The experimental angular distributions for the ^{14}N- ground state obtained in the $^{16}O(d, \alpha)^{14}N$ reaction at the following incident energies:-
(a) E_d ranged from 1.876 to 10.425 MeV.(b) E_d ranged from 13.304 to 14.9 MeV.
(c) E_d ranged from 15 to 18.1 MeV.(d) E_d ranged from 18.8 to 40 MeV.
(The errors for the experimental points in this figure are taken to be + or - 10 %.)**

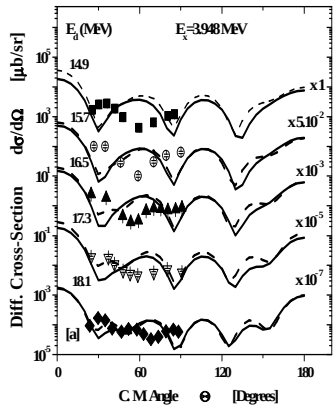

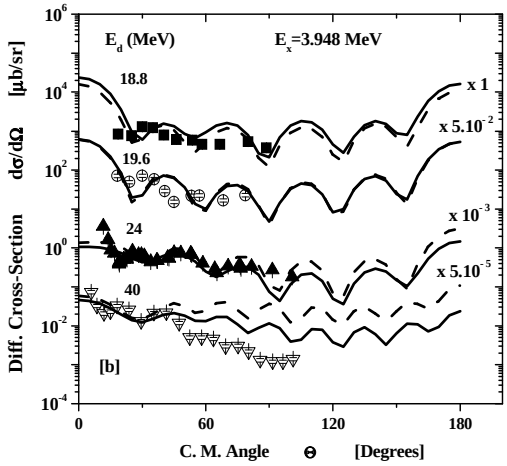

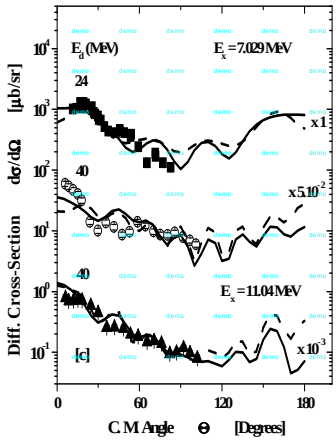

Figure: (2 B):
The experimental angular distributions for the ^{14}N-excited states obtained in the $^{16}O(d, \alpha)^{14}N$ reaction at the following incident energies:-
i) The lower ^{14}N-state 3.948 MeV at the incident energies:
a) E_d ranged from 14.9 to 18.1 MeV.
b) E_d ranged from 18.8 to 40 MeV.
ii) The two lower ^{14}N-states 7.029 and 11.04 MeV at the incident energies:
c) E_d = 24 and 40; and 40 MeV, respectively.
(The errors for the experimental points in this figure are taken to be + or - 10 %.)**

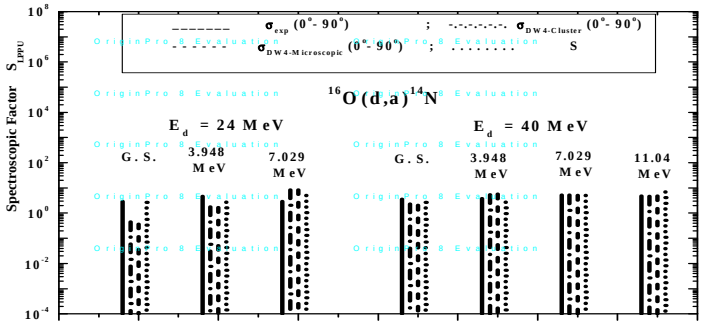

Fig. (3) :The fitting of experimental relative cross-sections σ_{exp} (0°-90°) for the lower ^{14}N-states G. S.; 3.948; 7.029 and 11.04 MeV at the incident energies 24 and 40 MeV with the integrirte theoretical cross-sections $\sigma_{Cluster}$ (0°-90°) -dashed-dotted-lines-; $\sigma_{Cluster}$ (0°-90°) -dashed-dotted-lines-; $\sigma_{Microscopic}$ (0°-90°) -short dashed-lines and the LPPU-spectroscopic factors S -dotted lines-.

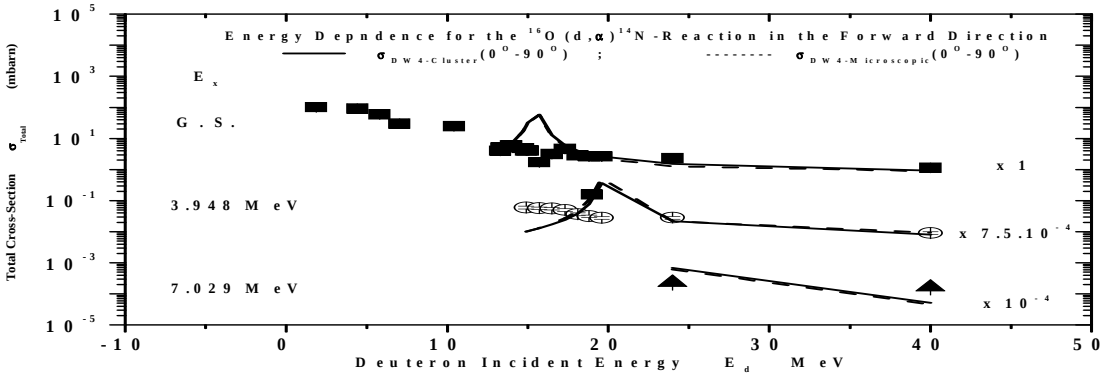

Fig. (4): The energy-dependence of the forward total cross-sections for the lowest three ^{14}N-states 0.0 (1^+; 0); 3.948 (1^+; 0) and 7.029 MeV (2^+; 0) obtained in the reaction $^{16}O(d,\alpha)^{14}N$. The errors for the experimental points in this figure are taken to be + or - 10 % .)

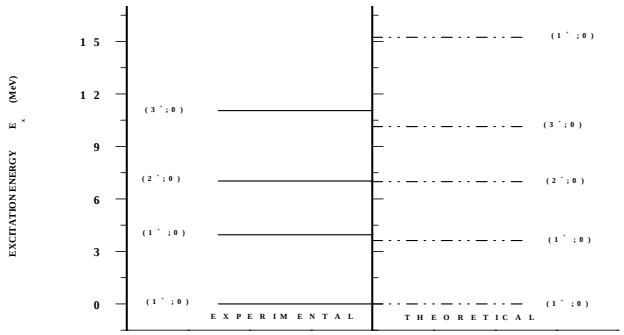

Fig. (5): Experimental and theoretical excitation energies for the first five states in the nucleus ^{14}N.